PREDICTION MODEL FOR CHANGE IN PERFORMANCE OF RUBBLE MOUND REVETMENT UNDER DAMAGE PROGRESSION

Takao Ota[1], Yoshiharu Matsumi[2], Hiroyuki Kawamura[3] and Kenichi Ohno[4]

In this study, the change characteristics of wave dissipation performance of rubble mound revetment under the damage progression of armor layer are investigated using a numerical wave flume and a series of model profiles for damaged armor layer. The reflection coefficient and wave overtopping rate are used as the performance measures. A number of irregular waves with different wave profiles and wave grouping properties are generated in the numerical wave flume to obtain many data of the performance measures. Secondly, an artificial neural network (ANN) model is applied to predict the change of the performance measures with the cumulative damage of armor layer. The three-layered neural network calibrated by the results of the numerical experiments can predict the reflection coefficient with sufficient accuracy and the overtopping rate reasonably well.

Keywords: rubble-mound revetment; cumulative damage of armor layer; numerical wave flume; artificial neural network

INTRODUCTION

The infrastructures are required to keep a certain level of performance during the in-service period. From this viewpoint, it is necessary to consider the deformation (damage) of structure and its influence on the performance retention for the long term. Moreover, it is needed to develop the prediction (evaluation) model for the cumulative damage and change of performance to make decision of repair or renewal. We have studied about the variation of wave dissipation performance of revetment due to damage of armor layer (Ota et al. 2010, 2012) and the prediction model for performance using an artificial neural network (ANN) (Hirayama et al. 2012). It was also pointed out that the combination of adjacent incident wave heights influenced wave overtopping. In this study, the change characteristics of performance of rubble mound revetment under the damage progression of armor layer are investigated using a numerical wave flume and a series of model profiles corresponding to the damage in the crest and seaward slope of the revetment. The reflection coefficient and wave overtopping rate are used as the performance measures. Because the combination characteristics of adjacent incident waves are important for wave overtopping especially as mentioned above, the wave grouping characteristics are also considered. A number of irregular wave trains with consideration for the wave grouping characteristics are generated in the numerical wave flume to obtain many data of the reflection coefficient and wave overtopping rate. Secondly, ANN is applied to predict the change of the reflection coefficient and wave overtopping rate associated with the cumulative damage of armor layer. ANN has been used to estimate wave overtopping in many studies (for example, Medina et al. 2002; Verhaeghe 2005; Mase et al. 2007) for the design of the coastal structures, however, few studies considered the effects of damage of armor layer on overtopping for the maintenance. In this study, the input data of ANN are the conditions of damage, revetment and wave, and the applicability of the prediction model is investigated.

IRREGULAR WAVE GENERATION IN NUMERICAL WAVE FLUME

To investigate the change of the reflection coefficient and wave overtopping rate and to create the

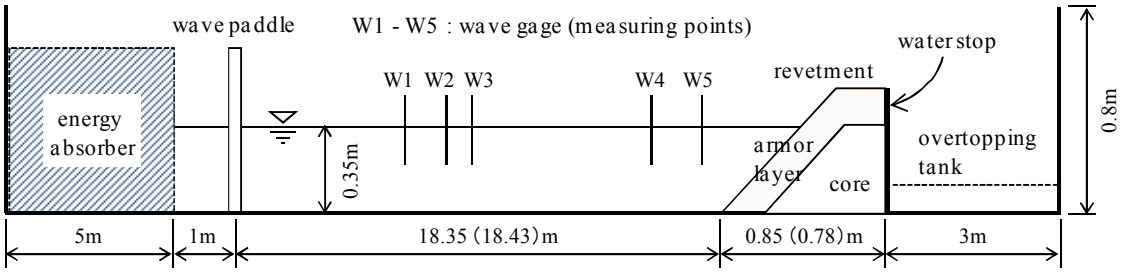

Figure 1. Schematic of computational domain

[1] Dept. of Social Systems Eng., Tottori Univ., 4-101 Koyama Minami Tottori 680-8552, Japan
[2] Dept. of Social Systems Eng., Tottori Univ., 4-101 Koyama Minami Tottori 680-8552, Japan
[3] Nishi-Nihon Branch, Sansyosuiko Inc., Hakata, Fukuoka, 812-0013, Japan
[4] University evaluation office, Tottori Univ., 4-101 Koyama Minami Tottori 680-8550, Japan

Table 1. Conditions and values of parameters for CADMAS-SURF

wave model		wave source
difference scheme		VP-DONOR 0.2
grid interval (cm)	vertical	1.0
	horizontal	3.0
armor layer	porosity	0.39
	inertia coefficient	1.2
	drag coefficient	1.0
core	porosity	0.37
	inertia coefficient	2.0
	drag coefficient	1.5

input and output data of the training and test data set for ANN, two dimensional numerical wave flume "CADMAS-SURF" (Coastal Development Institute of Technology 2001, 2008) V 5.1 was used in this study. The governing equations are the continuity equation and Navier-Stokes equation for incompressible and viscous fluid. The water surface variation is computed using the volume of fluid (VOF) method. Figure 1 shows the schematic of computational domain and this corresponds to the conditions of the former experiments that we conducted (Hirayama et al. 2012). A water stop and overtopping tank were set behind the revetment and the volume of overtopped water per unit width is computed from the increment of the VOF function F in the tank.

The modified Bretschneider-Mitsuyasu spectrum (BM) and JONSWAP spectrum (JO) with the shape parameter γ = 9.0 were used as the target energy spectrum for the incident irregular waves. JO with this value of γ was fairly narrowband in comparison with BM and was used to generate the irregular waves that had different wave grouping characteristics. As the input conditions for the wave, the significant wave period $T_{1/3}$ = 1.6 s and the significant wave height $H_{1/3}$ = 11 cm were used. The input value of $H_{1/3}$ was determined by the result of the calibration calculation without the structures and with the energy absorber at the right-hand edge of the flume. The value of $H_{1/3}$ was about 10 cm at the location of W5 shown in Figure 1 and the mean run lengths for BM and JO were 1.3 and 2.05 respectively for the computed irregular waves. The other conditions and values of parameters are shown in Table 1. A total of 15 irregular wave trains of 960 s (600 $T_{1/3}$) duration were generated for each spectrum by changing the initial value of random number for the component waves. Five measuring points W1-W5 corresponding to wave gages were placed to obtain the time series of the free surface elevation. The data at W1 - W3 were used to separate the incident and reflected waves using linear wave theory.

NUMERICAL EXPERIMENT ON WAVE REFLECTION AND OVERTOPPING

Model Profiles of Revetment

A rubble mound revetment was set on the flat bottom of wave flume as shown in Figure 1. The revetment consisted of a core and an armor layer whose characteristics were shown in Table 1. Figure 2(a) and (b) show the model profiles of damaged armor layer. The crest width was 10 cm and the

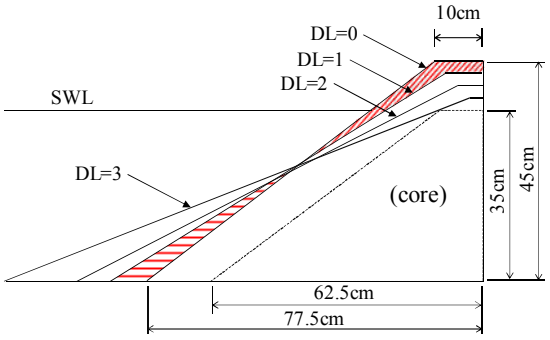

(a) *B*=10cm

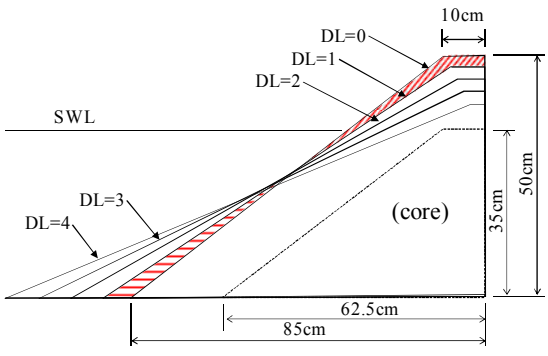

(b) *B*=15cm

Figure 2. Model profiles for damaged armor layer

heights B were 10 and 15 cm for the initial profile of the revetment. The seaward slope of the initial profile was 2:3. These model profiles corresponded to the damage in the crest and slope, and were determined by reference to the experimental results of Kubota et al. (2009). In these models, the crest height decreased ΔB = 2.5 cm as the damage level DL increased one. The crest width was reduced at the same rate for height decrease $\Delta B/B$. The seaward slope was determined so that the accumulated area was equal to the eroded area in the armor layer. In this study, four damaged profiles of ΔB = 0 – 7.5 cm (DL = 0 – 3) for the case of B = 10 cm, and five profiles of ΔB = 0 – 10 cm (DL = 0 – 4) for the case of B = 15 cm. The above-mentioned 15 irregular wave trains for each of two energy spectra were acted on the model revetments and the reflection coefficient and wave overtopping rate were obtained.

Variation of reflection coefficient and wave overtopping rate

As mentioned above, the reflection coefficient was obtained from the time series of the free surface elevation at three measuring points W1 – W3, and the overtopping quantity per unit width was computed from the area integral of the VOF function in the overtopping tank shown in Figure 1. Figure 3 shows the average and standard deviation of the reflection coefficient K_R and the mean overtopping rate (= mean overtopping quantity per unit width and time) q as a function of the damage level DL of the revetment. The open circle and the length of error bar in the figures denote the average and standard deviation respectively. Table 2 shows the variation coefficient for K_R and q. In the cases of same B, the

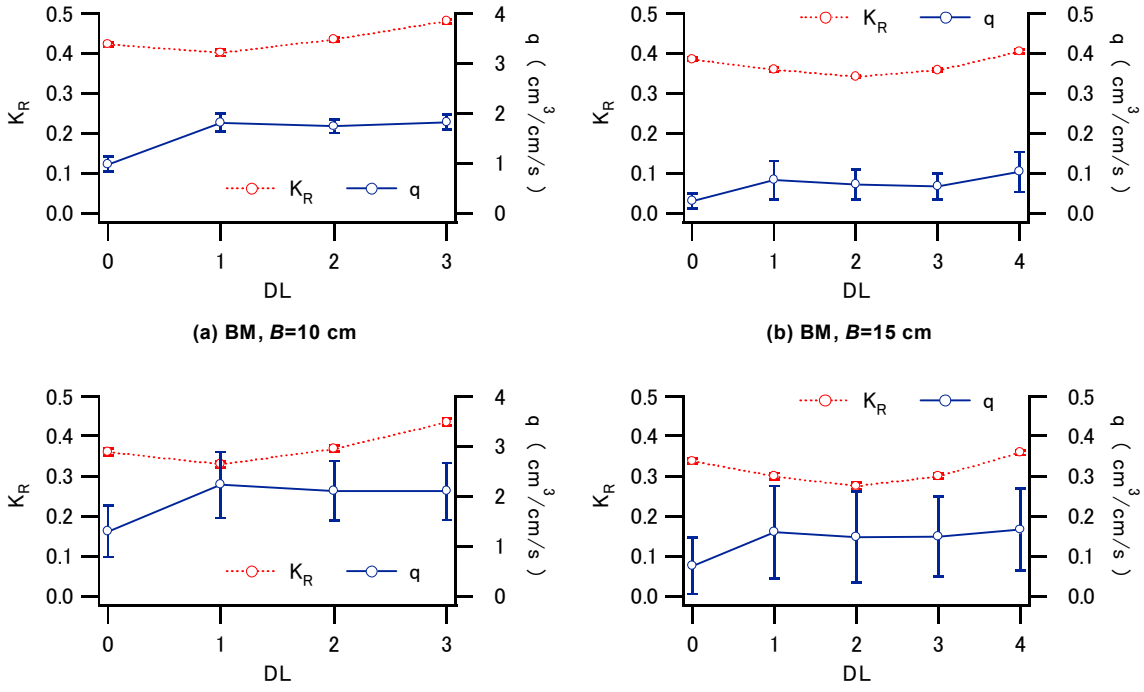

Figure 3. Variation of reflection coefficient and overtopping rate

Table 2. Variation coefficient for reflection coefficient and overtopping rate

spectrum	B (cm)	measure	variation coefficient				
			DL =0	1	2	3	4
BM	10	K_R	0.014	0.016	0.015	0.010	-
		q	0.153	0.099	0.082	0.081	-
	15	K_R	0.011	0.014	0.013	0.012	0.012
		q	0.664	0.567	0.500	0.487	0.484
JO	10	K_R	0.022	0.024	0.021	0.019	-
		q	0.395	0.296	0.283	0.272	-
	15	K_R	0.019	0.029	0.028	0.022	0.018
		q	0.951	0.723	0.773	0.680	0.619

tendencies of variation in the average of K_R and q are similar. As for K_R, the standard deviation and variation coefficient are small and the change tendencies are uniform in the 15 irregular wave trains. The averages of K_R decrease till DL = 1 and DL = 2 in the cases of B = 10 and 15 cm, and then they increase as the damage progresses. It is conceivable that the wave reflection is intensified by the exposed water stop in large DL.

As for q, the standard deviation and variation coefficient are widely different depending on the energy spectrum and B. In the case of B = 10 cm, the dispersion of q is small compared with the case of B = 15 cm because of the relatively large overtopping quantity and the change tendencies are nearly uniform in the 15 irregular wave trains. The overtopping quantity decreases to about tenth compared with the case of B = 10 cm and the change tendencies are not uniform. The standard deviation and the variation coefficient are larger in the case of JO and it appears that the influence of wave grouping makes the dispersion larger. In this connection, about five wave data whose overtopping quantity are large are picked up from each of the 15 irregular wave trains for the initial profile (DL = 0) using the data of free surface elevation at W5 and the VOF function in the overtopping tank. Figure 4 shows the comparison of the incident wave height H_2 that brings overtopping with the adjacent wave height H_1 obtained from the above data. In the case of JO whose mean run length is longer, H_1 is close to H_2 and it shows the wave grouping clearly. It is conceivable that the significant influence of the adjacent wave due to wave grouping makes the variation in overtopping rate larger. Figure 5 shows the overtopping quantity per wave and unit width Q as a function of the ratio of the adjacent incident wave heights H_1/H_2. In the case of JO, a lot of values of H_1/H_2 are in the range of 0.5 – 1.0 and the dispersion of Q is large compared with that of BM.

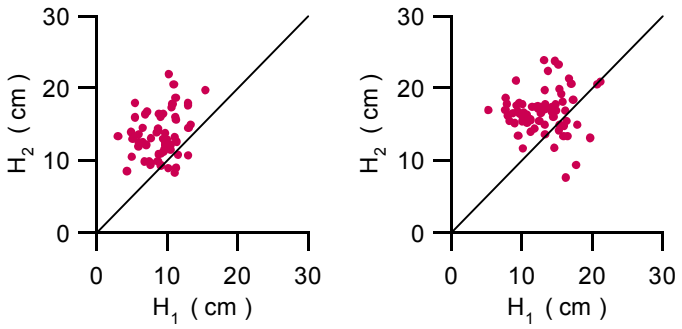

Figure 4. Comparison of wave height that brings overtopping with adjacent wave height

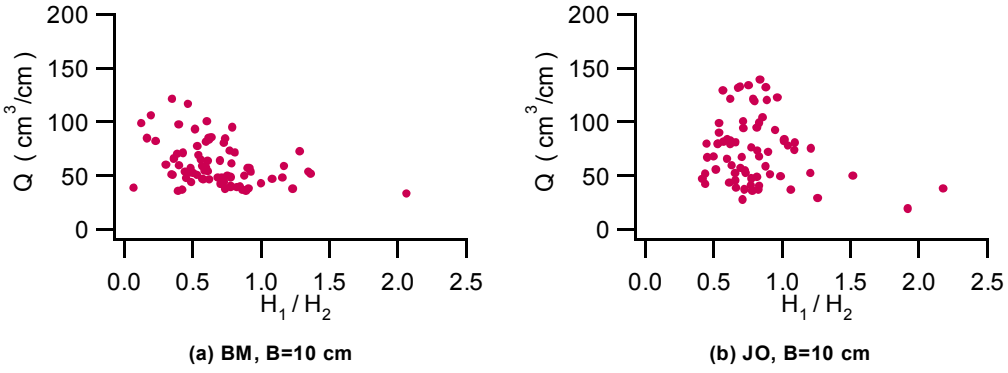

Figure 5. Relations between overtopping quantity and ratio of adjacent incident wave heights

PREDICTION MODEL USING ANN

The prediction model for the performance measures –reflection coefficient and overtopping rate- is made by using ANN. A three-layered ANN that consists of an input layer, one hidden layer and an output layer is employed in this study. Figure 6 shows the diagram of a three-layered ANN, where x_i is the input data, v_{ij} is the weight on pathways between input and hidden layer, θ_j is the threshold in units of hidden layer, f is the transfer function in units of hidden and output layer, w_j is the weight on pathways between hidden and output layer, and γ is the threshold in unit of output layer. As the transfer function, the tangent sigmoid function (output from -1 to 1) and the linear function (arbitrary output) are used for the units of hidden layer and output layer respectively.

The input data are the quantities concerned with the damage of armor layer (crest width, seaward slope of damaged profile, horizontal decrease rate and decrease rate of crest height $\Delta B/B$), the revetment (water depth at toe of revetment, crest height of initial profile, seaward slope of initial profile, porosity of armor layer, nominal diameter of armor stone and height of core) and the wave (significant wave height and period at W1 and mean run length at W1). A total of 13 data that are determined by reference to Hirayama et al. (2012) are used as the input data for ANN. The horizontal decrease rate of the armor layer was defined by Kubota et al. (2009) and it is given by the rate between the horizontal decrement of the armor layer at the still water level and the horizontal thickness of armor layer in the initial profile. The nominal diameter is 2.5 cm as Hirayama et al. (2012) used. The number of unit in the output layer is one, thus the output data is the reflection coefficient or the overtopping rate only. In other words, the ANNs are built for the prediction of the reflection coefficient and the overtopping rate respectively.

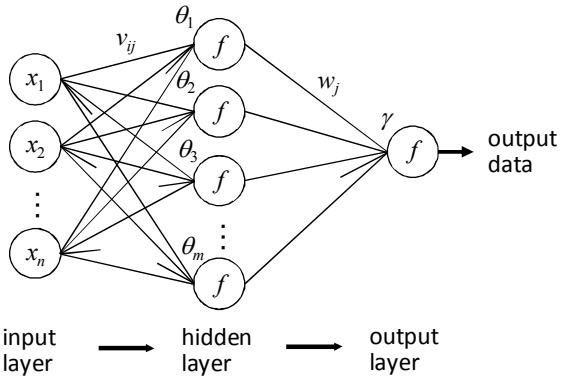

Figure 6. Diagram of a three-layered ANN

To build the ANN, the back-propagation training is used in this study. In this method, the parameters in the ANN (v_{ij}, θ_j , w_j and γ) are adjusted so as to minimize the error between the output data of the given data (training data) and the output of the network by the feedback of the error. The Levenberg-Marquart method is used as the back-propagation training algorithm. As the trials on the number of unit in the hidden layer, the ANNs are built with the unit number of 13, 18, 22 and 26 for the prediction of the reflection coefficient and the overtopping rate respectively. The training data are a set of input and output data corresponding to 13 irregular wave trains among the generated data by the numerical wave flume. Therefore, the numbers of training data set are basically 52 and 65 for the cases of B = 10 cm and B = 15 cm respectively. The remaining data of two irregular wave trains are used as the test data set to verify the prediction performance. The prediction models using ANN are built for the combination of the reflection coefficient and overtopping rate, BM and JO, B = 10 and 15 cm. Two more models are also built for the reflection coefficient and overtopping rate using the mixed training data of BM and JO in the case of B = 10 cm because the dispersion of the numerical results are relatively small as shown in Figure 3 and Table 2.

Figures 7 and 8 show the comparison of the output data in the test data set with the prediction results by the ANN in the case of BM and JO with B = 10 cm. The ANNs predict the reflection coefficient K_R within 5 % error including the other cases that are not shown in figure. The ANN whose number of the unit in the hidden layer is 13 gives the best prediction results for K_R. As for the overtopping rate q, the ANNs predict within about 25 % and 40 % error in the case of BM and JO. In the other cases, the prediction errors are about 50 % in the case of BM with B = 15 cm, and is larger in

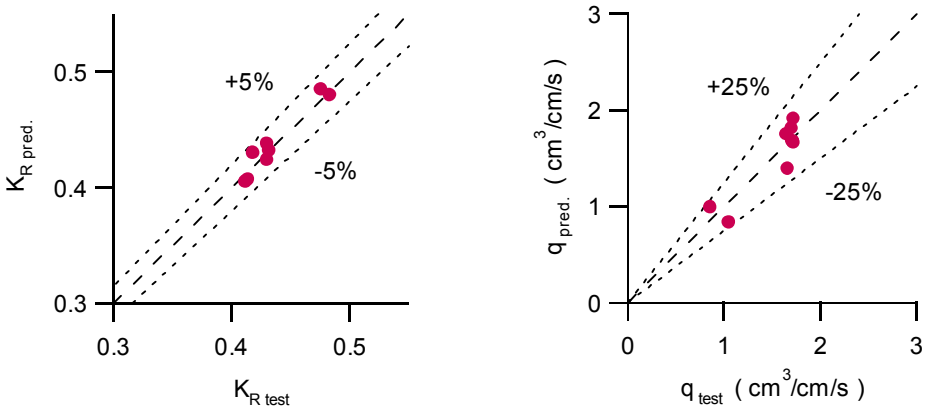

(a) Reflection coefficient **(b) Overtopping rate**

Figure 7. Comparison of test data with prediction result by ANN (BM, B=10cm, number of unit in hidden layer=13)

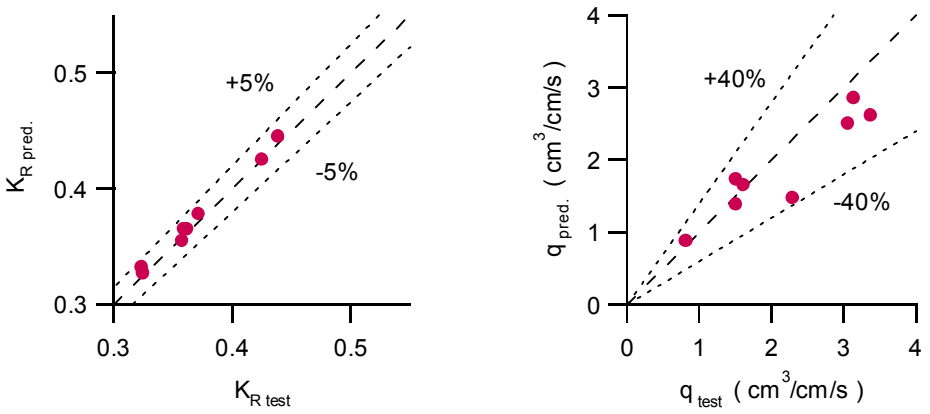

(a) Reflection coefficient **(b) Overtopping rate**

Figure 8. Comparison of test data with prediction result by ANN (JO, B=10cm, number of unit in hidden layer=13)

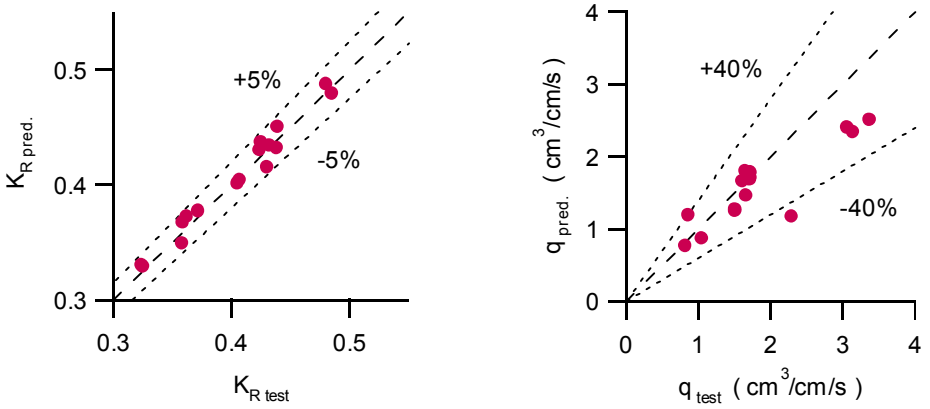

(a) Reflection coefficient **(b) Overtopping rate**

Figure 9. Comparison of test data with prediction result by ANN (mix of BM and JO, B=10cm, number of unit in hidden layer=13)

the case of JO with B = 15 cm. The ANN whose number of the unit in the hidden layer is 13 gives better prediction results for q. Figure 9 shows the prediction results in the case of the mixed data of BM and JO with B = 10 cm. The prediction errors are within 5 % for K_R and about 40 % for q. In both the reflection coefficient and overtopping rate, the prediction errors correspond to the values of variation coefficient shown in Table 2. Therefore, it is conceivable that the prediction models by ANN give the reasonable results for the reflection coefficient and overtopping rate even in the cases of large prediction error.

CONCLUSIONS

In this study, the change characteristics of wave dissipation performance (the reflection coefficient and wave overtopping rate) of rubble mound revetment under the damage progression of armor layer were investigated using a numerical wave flume and a series of model profiles for damaged armor layer. To obtain many data of the reflection coefficient and wave overtopping rate and consider the wave grouping characteristics that influence on the wave overtopping especially, a total of 15 irregular wave trains were generated for each of two energy spectra (modified Bretschneider-Mitsuyasu and JONSWAP) whose spectral bandwidth were fairly different. Based on the results of the numerical experiment, the prediction models using ANN were built for the reflection coefficient and wave overtopping rate. The input data for ANN were the conditions of the damage of armor layer, the revetment and the wave. The conclusions of this study are summarized as follows:

1. Variation of the reflection coefficient;

- The tendencies of variation in the average were similar in the cases of same initial crest height of the revetment.
- The dispersion due to difference of wave train was small in the same damage level of the revetment.

2. Variation of the wave overtopping rate;
   - The dispersion due to difference of wave train was large in the case of high crest of the revetment.
   - The dispersion was large in the case of narrowband spectrum. It is conceivable that the significant influence of the adjacent wave on the wave that brings overtopping due to wave grouping makes the variation in overtopping rate larger.
3. The ANN predicted the reflection coefficient within 5 % error, however, the errors were more than 25 % for the prediction of overtopping rate.

ACKNOWLEDGMENTS

The authors express our gratitude to Hiromichi Yoshiki for his contributions to the numerical experiments.

REFERENCES

Coastal Development Institute of Technology. 2001. *CADMAS-SURF*; *Its research and development*, 296pp. (in Japanese)

Coastal Development Institute of Technology. 2008. *CADMAS-SURF*; *Examples of practical calculation*, 306pp. (in Japanese)

Hirayama, T., H. Fujimoto, Y. Matsumi, T. Ota and K. Ohno. 2012. Evaluation system for change of wave overtopping under damaged armour layers around top of slope-type revetment, *Journal of Japan Society of Civil Engineers, Ser. B3* (*Ocean Engineering*), Vol. 68, No. 2, I_330-I_335. (in Japanese)

Kubota, S., M. Yamamoto, A. Matsumoto and M. Hanzawa. 2009. An experimental study on deformation of wave-dissipating concrete blocks covering caisson breakwaters, *Journal of Coastal Engineering*, JSCE, Vol. 56, 906-910. (in Japanese)

Mase, H., M.T. Reis, S. Nagahashi, T. Saitoh and T.S. Hedges. 2007. Effects of zero-overtopping data in artificial neural network predictions, *Proceedings of the 5th Coastal Structures International Conference, CSt07*, 1542-1551.

Medina, J.R., Gonzalez-Escriva, J.A., Garrido, J.M. and De Rouck, J. 2002. Overtopping analysis using neural networks, *Proceedings of the 28th International Conference on Coastal Engineering*, ASCE, 2165-2177.

Ota, T., Y. Matsumi, T. Hirayama and A. Kimura. 2010. Models for profile change of rubble mound revetment and performance evaluation, *Proceedings of the International Conference on Coastal Engineering*, No. 32, Paper #: structures.38. Retrieved from https://journals.tdl.org/icce/index.php/icce

Ota, T., Y. Matsumi, N. Kato and K. Ohno. 2012. Modeling of damage progression of rubble mound revetment and application to performance evaluation, *Proceedings of the International Conference on Coastal Engineering*, No. 33, Paper #: structures.49. Retrieved from https://journals.tdl.org/icce/index.php/icce

Verhaeghe, H., 2005, Neural network prediction of wave overtopping at coastal structure, Doctorate Dissertation to Department of Civil Engineering, Ghent University.